

# Polarization Modulation by free-Standing Asymmetric Hole Arrays

Hong-Wen Hsieh and Shun-Tung Yen

**Abstract**—We theoretically demonstrate modulation of light polarization by a crossed rectangular hole array with asymmetric arm lengths. There are two waveguide modes that can modulate the  $x$ - and  $y$ - polarized incident waves independently. A specific structure is proposed to convert a left-hand incident wave to a right-hand outgoing wave by transmission.

**Keywords**—Crossed rectangular hole array, extraordinary optical transmission, polarization modulation.

## I. INTRODUCTION

TRANSMISSION properties of two-dimensional grating structure have been extensively studied since Ebbesen *et al.* found the peculiar optical transmission of periodically perforated metallic film in 1998 [1]. Investigations have been made on the transmission behavior of apertures of various shapes, such as square [2], rectangular [3], circular [4], and even crossed rectangular [5] ones. Among them, we are interested especially in the crossed rectangle because of its flexibility in geometrical profile in design. The crossed rectangular array has shown a good performance in optically filtering [6]. We expect that it can also behave as a good polarization modulator by properly designing the geometric shape. In this paper, we theoretically demonstrate that the polarization can be modulated after the light transmits through an asymmetric crossed rectangular hole array. With particular geometry design, a quarter-wave or a half-wave modulation can be achieved.

## II. CALCULATION APPROACHES

Figure 1 shows schematically the hole array which we consider in this work. The whole space is separated into three regions as shown in Fig. 1(a). Regions I ( $0 \leq z$ ) and III ( $z \leq L_d$ ) are semi-infinite free spaces. The wave is incident from Region I and transmitted through Region II into Region III. Region II ( $0 \leq z \leq L_d$ ) is a periodically perforated metal layer. The metal in Region II is assumed to be perfectly conducting and there is no dielectric material inside the hole. The lattice constants for the  $x$ - and  $y$ -directions are  $L_x$  and  $L_y$ , respectively. We focus on the square lattice, i.e.  $L_x = L_y$ . The lengths of vertical and horizontal arms of each crossed rectangle are denoted by  $L_v$  and  $L_h$ , and the widths of the two

arms are both equal to  $L_w$ , as shown in Fig. 1(b). The thickness of the metallic film is  $L_d$ . Our calculation is based on the basis expansion method similar to [7]. In this calculation, we only focus on in-plane components of EM field; the in-plane electric field in the free space region is expanded by  $s$ - and  $p$ - polarized plane waves:

$$\mathbf{E}_{smn} = \frac{1}{\sqrt{L_x L_y (k_{xm}^2 + k_{yn}^2)}} \begin{pmatrix} k_{yn} \\ -k_{xm} \end{pmatrix} \exp(ik_{xm}x + k_{yn}y), \quad (1a)$$

$$\mathbf{E}_{pmn} = \frac{1}{\sqrt{L_x L_y (k_{xm}^2 + k_{yn}^2)}} \begin{pmatrix} k_{xm} \\ k_{yn} \end{pmatrix} \exp(ik_{xm}x + k_{yn}y), \quad (1b)$$

where  $m$  and  $n$  are integers,  $k_{xm} = k_{x0} + 2\pi m/L_x$  and  $k_{yn} = k_{y0} + 2\pi n/L_y$ ,  $k_{x0}$  and  $k_{y0}$  are the  $x$ - and  $y$ -directional components of the incident wave vector  $k_0$ . For magnetic fields, we use  $\hat{z} \times \mathbf{H}_{smn}$  and  $\hat{z} \times \mathbf{H}_{pmn}$  instead of  $\mathbf{H}_{smn}$  and  $\mathbf{H}_{pmn}$ , because they can easily be expressed as  $\hat{z} \times \mathbf{H}_{smn} = -Y_{smn} \mathbf{E}_{smn}$  and  $\hat{z} \times \mathbf{H}_{pmn} = -Y_{pmn} \mathbf{E}_{pmn}$ , where  $Y_{smn} = k_{zmn}/k_0$ ,  $Y_{pmn} = k_0/k_{zmn}$ , and  $k_{zmn} = \sqrt{k_0^2 - (k_{xm}^2 + k_{yn}^2)}$ . The total electric fields in Regions I and III can be written as:

$$\mathbf{E}^I = \sum_{\sigma mn} \mathbf{E}_{\sigma mn} \{a_{\sigma mn}^I \exp(ik_{zmn}z) + b_{\sigma mn}^I \exp(-ik_{zmn}z)\}, \quad (2a)$$

$$\mathbf{E}^{III} = \sum_{\sigma mn} \mathbf{E}_{\sigma mn} \{a_{\sigma mn}^{III} \exp[ik_{zmn}(z - L_d)] + b_{\sigma mn}^{III} \exp[-ik_{zmn}(z - L_d)]\}. \quad (2b)$$

Also, for the magnetic fields,

$$\hat{z} \times \mathbf{H}^I = \sum_{\sigma mn} \hat{z} \times \mathbf{H}_{\sigma mn} \{a_{\sigma mn}^I \exp(ik_{zmn}z) - b_{\sigma mn}^I \exp(-ik_{zmn}z)\}, \quad (3a)$$

$$\hat{z} \times \mathbf{H}^{III} = \sum_{\sigma mn} \hat{z} \times \mathbf{H}_{\sigma mn} \{a_{\sigma mn}^{III} \exp[ik_{zmn}(z - L_d)] - b_{\sigma mn}^{III} \exp[-ik_{zmn}(z - L_d)]\}, \quad (3b)$$

where  $a_{\sigma mn}^I$  and  $b_{\sigma mn}^I$  are the expansion coefficients in Region I; similarly,  $a_{\sigma mn}^{III}$  and  $b_{\sigma mn}^{III}$  are the expansion coefficients in Region II.  $\sigma$  denotes the  $s$ - and  $p$ -polarization. The EM field inside the hole region is expanded by the eigenmodes of the crossed rectangular waveguide obtained from [8]. Denoting the crossed rectangular waveguide modes by  $\mathbf{E}_\lambda$ , we can write the fields inside the hole as

$$\mathbf{E}^{II} = \sum_\lambda \mathbf{E}_\lambda \{a_\lambda^{II} \exp(ik_{z\lambda}z) + b_\lambda^{II} \exp[-ik_{z\lambda}(z - L_d)]\}, \quad (4)$$

and

Hong-Wen Hsieh and Shun-Tung Yen are with the Department of Electronics Engineering and Institute of Electronics, National Chiao Tung University, Hsinchu, Taiwan, Republic of China (phone: +886-03-5712121-54235; e-mail: hsieh0314@gmail.com, styen@cc.nctu.edu.tw ).

$$\hat{z} \times \mathbf{H}^II = \sum_{\lambda} \hat{z} \times \mathbf{H}_{\lambda} \left\{ a_{\lambda}^{II} \exp(ik_{z\lambda} z) - b_{\lambda}^{II} \exp[-ik_{z\lambda} (z - L_d)] \right\}, \quad (5)$$

with  $\hat{z} \times \mathbf{H}_{\lambda} = -Y_{\lambda} \mathbf{E}_{\lambda}$ , where  $a_{\lambda}^{II}$  and  $b_{\lambda}^{II}$  are the expansion coefficients,  $Y_{\lambda} = k_{z\lambda}/k_0$  for TE waveguide modes and  $Y_{\lambda} = k_0/k_{z\lambda}$  for TM waveguide modes,  $k_{z\lambda} = \sqrt{k_0^2 - \gamma_{\lambda}^2}$  and  $\gamma_{\lambda}$  is the cutoff wavenumber of the modes.

To find the expansion coefficients, we match the EM fields at the two interfaces using the boundary conditions  $\mathbf{E}^I(z=0) = \mathbf{E}^{II}(z=0)$  and  $\mathbf{E}^{III}(z=L_d) = \mathbf{E}^{II}(z=L_d)$  for the electric fields. Multiplying  $\mathbf{E}_{\sigma mn}$  on both sides of the two equations and integrating over a unit cell, we obtain the following matrix equations:

$$\mathbf{A}^I + \mathbf{B}^I = \mathbf{M}(\mathbf{A}^{II} + \mathbf{B}^{II} \mathbf{D}), \quad (6)$$

$$\mathbf{A}^{III} + \mathbf{B}^{III} = \mathbf{M}(\mathbf{A}^{II} \mathbf{D} + \mathbf{B}^{II}), \quad (7)$$

where  $\mathbf{A}^I$ ,  $\mathbf{B}^I$ ,  $\mathbf{A}^{II}$ ,  $\mathbf{B}^{II}$ ,  $\mathbf{A}^{III}$ , and  $\mathbf{B}^{III}$  are column vectors with the expansion coefficients as elements. The matrix  $\mathbf{M}$  have elements  $M_{\sigma mn, \lambda} = \int_0^{L_x} dx \int_0^{L_y} dy \mathbf{E}_{\sigma mn}^* \mathbf{E}_{\lambda}$ .  $\mathbf{D}$  is a diagonal matrix whose diagonal elements are  $\exp(ik_{z\lambda} L_d)$ . For the magnetic fields, we use the boundary conditions  $\hat{z} \times \mathbf{H}^I(z=0) = \hat{z} \times \mathbf{H}^{II}(z=0)$  and  $\hat{z} \times \mathbf{H}^{III}(z=L_d) = \hat{z} \times \mathbf{H}^{II}(z=L_d)$  in the hole region. Multiplying  $\mathbf{E}_{\lambda}$  on both sides of the two equations and integrating over only the hole region, we obtain

$$\mathbf{M}^{\dagger} \mathbf{Y}^I (\mathbf{A}^I - \mathbf{B}^I) = \mathbf{Y}^{II} (\mathbf{A}^{II} - \mathbf{B}^{II} \mathbf{D}), \quad (8)$$

$$\mathbf{M}^{\dagger} \mathbf{Y}^{III} (\mathbf{A}^{III} - \mathbf{B}^{III}) = \mathbf{Y}^{II} (\mathbf{D} \mathbf{A}^{II} - \mathbf{B}^{II}), \quad (9)$$

where  $\mathbf{Y}^I$ ,  $\mathbf{Y}^{II}$ , and  $\mathbf{Y}^{III}$  are diagonal matrices with diagonal elements  $Y_{\sigma mn}$  (for Regions I and III) and  $Y_{\lambda}$  (for Region II).

Combining (6)-(9), we can obtain

$$\begin{pmatrix} \mathbf{M}^{\dagger} \mathbf{Y}^I \mathbf{M} + \mathbf{Y}^{II} & (\mathbf{M}^{\dagger} \mathbf{Y}^I \mathbf{M} - \mathbf{Y}^{II}) \mathbf{D} \\ (\mathbf{M}^{\dagger} \mathbf{Y}^{III} \mathbf{M} - \mathbf{Y}^{II}) \mathbf{D} & \mathbf{M}^{\dagger} \mathbf{Y}^{III} \mathbf{M} + \mathbf{Y}^{II} \end{pmatrix} \begin{pmatrix} \mathbf{A}^{II} \\ \mathbf{B}^{II} \end{pmatrix} = 2 \begin{pmatrix} \mathbf{M}^{\dagger} \mathbf{Y}^I \mathbf{A}^I \\ \mathbf{M}^{\dagger} \mathbf{Y}^{III} \mathbf{B}^{III} \end{pmatrix}. \quad (10)$$

The coefficient column vectors  $\mathbf{A}^I$  and  $\mathbf{B}^{III}$  associated with the incoming waves are regarded as the given input. The other column vectors for the coefficients of outgoing waves can be obtained immediately by (10), (6), and (7). In this paper, we consider the case of normal incidence of a plane wave from Region I ( $k_{x0} = k_{y0} = 0$ ); In this case,  $\mathbf{B}^{III} = 0$  and the nonzero elements of  $\mathbf{A}^I$  are only  $a_{s00}^I$  and  $a_{p00}^I$  which are the coefficients of the modes  $\vec{E}_{s00} = (1, 0)^T / \sqrt{L_x L_y}$  and  $\vec{E}_{p00} =$

$$(0, 1)^T / \sqrt{L_x L_y}. \text{ The zero-order transmittance is thus } T = \left( |a_{s00}^{III}|^2 + |a_{p00}^{III}|^2 \right) / \left( |a_{s00}^I|^2 + |a_{p00}^I|^2 \right) \quad (10)$$

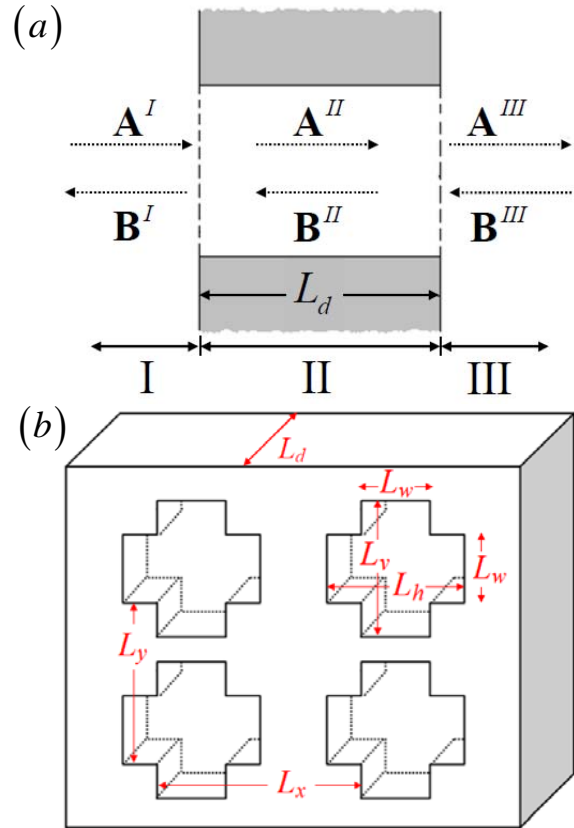


Fig. 1 Geometric profile of hole array. The notations are described in the text. (a) side-view (b) front-view

### III. RESULTS AND DISCUSSION

Among the waveguide modes, there are two modes which play crucial roles in the transmission process. The field patterns of the two modes are shown in Fig. 2(a) and (b). We denote the mode by the  $TE_x$  ( $TE_y$ ) mode if its dominant polarization is along  $x$  ( $y$ ). An  $x$ -polarized normal incident wave can transmit through the perforated film by exciting the  $TE_x$  mode because of the similarity in polarization. Similarly, a  $y$ -polarized wave can transmit through the film because of the presence of the  $TE_y$  mode. The cutoff frequency of the  $TE_x$  ( $TE_y$ ) mode can be approximated by that of the fundamental mode of an  $L_w \times L_v$  ( $L_w \times L_h$ ) rectangular waveguide, which corresponds to the cutoff wavenumber of  $\pi/L_v$  ( $\pi/L_h$ ). The field of the  $TE_x$  ( $TE_y$ ) mode concentrates mainly along the vertical (horizontal) arm, similar to the field of the fundamental mode of the  $L_w \times L_v$  ( $L_w \times L_h$ ) rectangular waveguide. This indicates that the transmission properties of the crossed rectangular array can be approximated by those of individual rectangular arrays. The transmission properties of the incident waves can be understood from those of the two waveguide modes  $TE_x$  and  $TE_y$ .

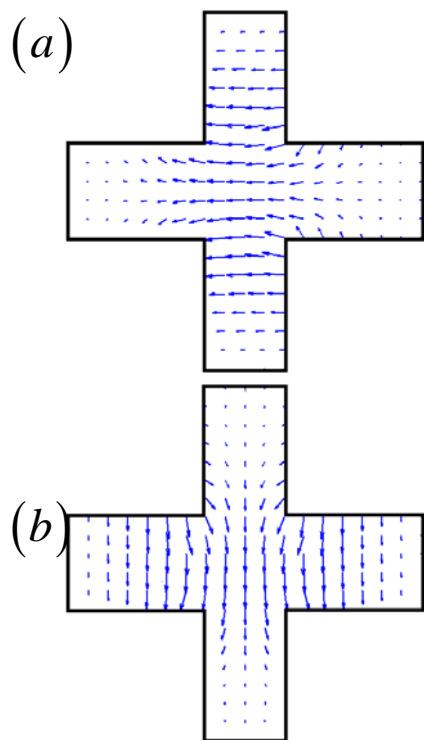


Fig. 2 (a) Field pattern of the  $TE_x$  waveguide mode. The mode is dominated by  $x$ -directional field and mainly concentrates in the vertical arm. (b) Field pattern of the  $TE_y$  waveguide mode. This mode, on the other hand, is dominated by  $y$ -directional field and mainly concentrates in the horizontal arm

For a symmetric crossed rectangular array ( $L_v = L_h$ ), the  $TE_x$  and  $TE_y$  modes are degenerate. The fields of the two modes can be transformed to one another by a rotation of 90 degree. In this case, the transmission properties of the  $x$ - and  $y$ - polarized normal incident waves are the same. When one of the arm lengths is reduced, the  $TE_x$  and  $TE_y$  modes are no longer degenerate. If we reduce  $L_v$ , the cutoff frequency of  $TE_x$  increases. Similarly, the cut-off frequency of the  $TE_y$  mode can be varied by changing  $L_h$ . Figure 3 shows the calculation transmittance for the  $x$ - and  $y$ - polarized normal incident waves. The geometric parameters used in the calculation are  $L_x = L_y = 96 \mu\text{m}$ ,  $L_v = 60 \mu\text{m}$ ,  $L_h = 80 \mu\text{m}$ ,  $L_w = 20 \mu\text{m}$ , and  $L_d = 64 \mu\text{m}$ . The transmission behaves differently for the different polarizations because of the geometric asymmetry. The transmission peaks in Fig. 3(a) arise from constructive interference between the forward-traveling and the backward-traveling waveguide modes. The lowest-frequency peak corresponds to the zero-order constructive interference at the cutoff frequency of the  $TE_x$  ( $TE_y$ ) mode for the  $x$ - ( $y$ -) polarized incident wave. In this asymmetric case, the  $y$ -polarized wave has the resonant peak at a lower frequency because of its longer arm length  $L_h$ . Figure 3(b) shows the phase of transmission spectrum. Because of the difference in cutoff which results in the difference in the propagation constant between the  $TE_x$  and  $TE_y$  modes, the phase change of the incident waves with different polarizations. The phase change of  $TE_x$  mode is larger than that of  $TE_y$  mode, because  $TE_x$  mode has a

lower cutoff frequency and a larger propagation constant. In brief, the asymmetric crossed hole array can give significant anisotropy in the transmission magnitude and phase change.

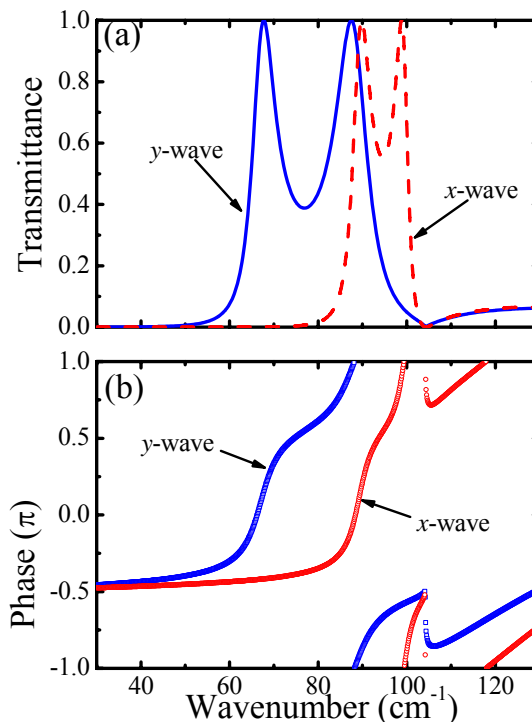


Fig. 3 (a) The transmittance of  $x$ -polarized (dotted line) and  $y$ -polarized (solid line) normal incident waves. The  $x$ -wave ( $y$ -wave) transmittance is calculated by  $T = |a_{s00}^m|^2 / |a_{s00}^i|^2$  ( $T = |a_{p00}^m|^2 / |a_{p00}^i|^2$ ). (b) The phase change by transmission through the array layer for the  $x$ - and  $y$ -polarized incident waves. For  $x$ -wave ( $y$ -wave), the phase change is obtained by the phase of  $a_{s00}^m / a_{s00}^i$  ( $a_{p00}^m / a_{p00}^i$ )

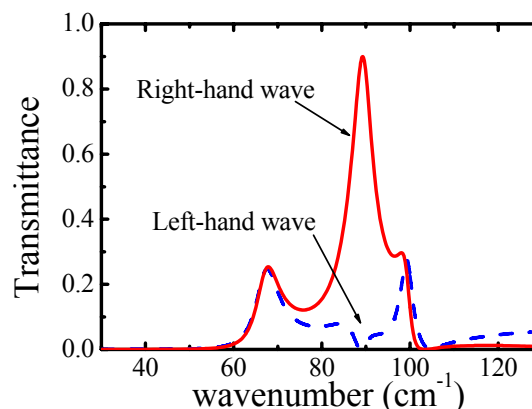


Fig. 4 Left- and right-handed transmitted components for a left-handed wave incidence. After passing through the array layer, the polarization is almost be "inverted"

The asymmetric hole array can be used to rotate the polarization of the wave. Figure 4 shows the spectra of the left-handed and the right-handed components of the transmitted wave for an normal incident wave with a purely left-handed polarization. Interestingly, the right-handed component

predominates in the transmitted wave. At the wavenumber of  $89 \text{ cm}^{-1}$ , the wave contains 99% of the right-handed component. This means that the phase of the wave is shifted by 180 degree by the transmission.

#### IV. CONCLUSION

In summary, we have shown significant modulations of the phase and the magnitude of the wave by the asymmetric crossed rectangular hole array. By proper design, we can obtain a quarter-wave plate or a half-wave plate operating at the frequency we desire. Such devices are particularly promising in the terahertz region because of easy fabrication by lithography.

#### ACKNOWLEDGMENT

The work was supported by National Nano Device Laboratory and National Science Council of the Republic of China under Contract No. NSC 98-2221-E-009-179.

#### REFERENCES

- [1] T. W. Ebbesen, H. J. Lezec, H. F. Ghaemi, T. Thio, and P. A. Wolff, "Extraordinary optical transmission through sub-wavelength hole arrays," *Nature* (London), vol. 391, pp.667-669, Feb 1998.
- [2] L. Martin-Moreno, F. J. Garcia-Vidal, H. J. Lezec, K. M. Pellerin, T. Thio, J. B. Pendry, and T. W. Ebbesen, "Theory of Extraordinary Optical Transmission through Subwavelength Hole Arrays," *Phys. Rev. Lett.*, vol. 86, no. 6, pp. 1114-1117, Feb 2001.
- [3] K. J. Klein Koerkamp, S. Enoch, F. B. Segerink, N. F. van Hulst and L. Kuipers, "Strong Influence of Hole Shape on Extraordinary Transmission through Periodic Arrays of Subwavelength Holes," *Phys. Rev. Lett.*, vol. 92, no. 18, pp. 183901-1-183901-4, May 2004.
- [4] F. J. Garcia de Abajo, R. Gomez-Medina, and J. J. Saenz, "Full transmission through perfect-conductor subwavelength hole arrays," *Phys. Rev. E.*, vol. 72, no. 1, pp. 016608-1-016608-4, Jul 2005.
- [5] Chia-Yi Chen, Ming-Wei Tsai, Tzu-Hung Chuang, Yi-Tsung Chang, and Si-Chen Lee, "Extraordinary transmission through a silver film perforated with cross shaped hole arrays in a square lattice," *Appl. Phys. Lett.*, vol. 91, pp. 063108-1-063108-3, Aug 2007.
- [6] Yong Ma, A. Khalid, Timothy D. Drysdale, and David R. S. Cumming, "Direct fabrication of terahertz optical devices on low-absorption polymer substrates," *Opt. Lett.*, vol. 34, no. 10, pp. 1555-1557, May 2009.
- [7] R. C. Compton, R. C. McPhedran, G. H. Derrick, and L. C. Botten, "Diffraction properties of a bandpass grid," *Infrared Phys.*, vol. 23, no. 5, pp. 239-245, Sep 1983.
- [8] F. L. Lin, "Modal Characteristics of Crossed Rectangular Waveguides," *IEEE Trans. Microwave Theory Tech.*, vol. MTT-25, no. 9, pp. 756-763, Sep 1977.